

UCLA

UCLA Previously Published Works

Title

Radiolabelling diverse positron emission tomography (PET) tracers using a single digital microfluidic reactor chip

Permalink

<https://escholarship.org/uc/item/44r9z66x>

Journal

Lab on a Chip, 14(5)

ISSN

1473-0197

Authors

Chen, Supin
Javed, Muhammad Rashed
Kim, Hee-Kwon
[et al.](#)

Publication Date

2014-03-07

DOI

10.1039/c3lc51195b

Peer reviewed

Radiolabelling diverse positron emission tomography (PET) tracers using a single digital microfluidic reactor chip

Supin Chen,^{*a} Muhammad Rashed Javed,^{bc} Hee-Kwon Kim,^{bc‡} Jack Lei,^{bc} Mark Lazari,^{abc} Gaurav J. Shah,^{bcd} R. Michael van Dam,^{abc} Pei-Yuin Keng,^{bc} and Chang-Jin "CJ" Kim^{ae}

^a *Bioengineering Department, University of California, Los Angeles, CA 90095, USA. Fax: 1(310)825-0267; Tel: 1(310)825-3977; *E-mail: supin.chen@engineering.ucla.edu*

^b *Molecular and Medical Pharmacology, University of California, Los Angeles, CA 90095, USA*

^c *Crumpp Institute for Molecular Imaging, University of California, Los Angeles, CA 90095, USA*

^d *Sofie Biosciences, Culver City, CA 90230, USA*

^e *Mechanical and Aerospace Engineering, University of California, Los Angeles, CA 90095, USA*

[‡]*Current affiliation: Department of Nuclear Medicine, Molecular Imaging & Therapeutic Medicine Research Center, Biomedical Research Institute, Chonbuk National University Medical School and Hospital, Jeonju, Jeonbuk 561-712, South Korea*

Abstract

Radiotracer synthesis is an ideal application for microfluidics because only nanogram quantities are needed for positron emission tomography (PET) imaging. Thousands of radiotracers have been developed in research settings but only a few are readily available, severely limiting the biological problems that can be studied *in vivo* via PET. We report the development of an electrowetting-on-dielectric (EWOD) digital microfluidic chip that can synthesize a variety of ¹⁸F-labeled tracers targeting a range of biological processes by confirming complete syntheses of four radiotracers: a sugar, a DNA nucleoside, a protein labelling compound, and a neurotransmitter. The chip employs concentric multifunctional electrodes that are used for heating, temperature sensing, and EWOD actuation. All of the key synthesis steps for each of the four ¹⁸F-labeled tracers are demonstrated and characterized with the chip: concentration of fluoride ion, solvent exchange, and chemical reactions. The obtained fluorination efficiencies of 90-95% are comparable to, or greater than, those achieved by conventional approaches.

Introduction

Positron emission tomography (PET) is a non-invasive imaging technique for quantification of biomolecular processes through detection of gamma rays arising from the annihilation of a positron (emanated from a radiotracer) and an electron [1]. A radiotracer is a biochemical compound tagged with a short-lived radionuclide, and the type of radiotracer determines the specific biological function that can be quantified via PET: sugars for monitoring metabolism, nucleic acids for examining cell replication, and neurotransmitters for studying brain activity. The ability to capture these molecular functions make PET a powerful medical tool used for diagnosing disease (like cancer and Alzheimer's disease), monitoring treatment, and developing pharmaceuticals [2].

Fluorine-18 is an ideal radioisotope for PET imaging because it emits a low energy positron, has a shorter positron range compared to other positron-emitters, decays to an innocuous ^{18}O , and has a moderate half-life that is long enough for chemical synthesis, transport to imaging clinic, and imaging molecules *in vivo* [3]. The fluorine atom can also be labelled onto many biomolecules because it is bioisostere to oxygen and can often substitute for a hydroxyl group or replace a hydrogen atom bound to a carbon atom [4]. More than 1,400 fluorine-18 radiotracers have been developed in research settings for imaging biological processes [5], but only a handful are commercially available. Production of radiotracers is limited by large capital investment in equipment and infrastructure, high operating costs, and short tracer lifetime [6]. Recently, there has been a movement towards technologies for decentralizing PET radiotracer production, in which imaging centers synthesize their own radiotracers onsite after receiving radioisotopes from radiopharmacies. For that reason, commercial automated synthesizers (e.g., Siemens Explora® One, Eckert & Ziegler Modular-Lab Standard, and GE FASTlab) were for flexible synthesis of various PET radiotracers using one machine [7]. However, these systems may require manual reconfiguration to synthesize different radiotracers [8] and must be operated within expensive and bulky hot cells (special chemical fume hoods that are surrounded by lead to provide radiation shielding).

Miniaturization by microfluidic systems is of direct interest for radiotracer development because of the substantial savings from both using less lead shielding and reducing use of expensive reagents. Reaction efficiency can also be improved with reduced volumes because of increased concentration of the radioisotope, expedited heat transfer, and quicker mass transport [3]. This is important for radiosynthesis reactions that sometimes involve low-yields and short half-life isotopes [4]. While the small amount of product limits the utility of microfluidic chemical synthesis in some cases, it is not an issue for PET imaging, which requires product in only nanogram quantities. Several microfluidic systems have been developed for radiotracer synthesis, including flow-through systems

and elastomer batch-flow reactors [9,10]. A commercial microfluidic reactor, the Advion NanoTek®, has also been used for radiotracer synthesis. It incorporates distribution valves, syringe pumps, pressure sensors, and heated vials to store and deliver reagents, concentrate radioisotopes, and control reactions [11]. The NanoTek® can transfer liquid volumes as small as 100 μL through a 16 μL capillary reactor and has been used to synthesize [^{18}F]fluoro-2-deoxy-D-glucose ([^{18}F]FDG) in 3 minutes with 62% yield [12].

A new and promising microfluidic approach of digital microfluidics [13,14,15] does not require mechanical valves, pumps, or channels, but instead uses electric potentials to manipulate liquids through the mechanism of electrowetting-on-dielectric (EWOD) [16]. Past reports have demonstrated a range of droplet functions (i.e., generating, moving, splitting, and merging) [17], precise control of droplet volumes [18], on chip liquid composition measurement [19], and suitability for multiple reagent chemical synthesis [20]. Our group has recently reported the use of EWOD for the synthesis of the most commonly used PET radiotracer, [^{18}F]FDG [21].

The EWOD-driven digital microfluidics has key advantages for radiotracer synthesis. Because droplet movement is electronically controlled without valves, pumps or tubes, liquid pathways can be defined in software, enabling diverse chemical synthesis processes to be carried out with just one type of EWOD chip. Since the sidewalls of channels are not necessary, an EWOD chip can be open to air, as first demonstrated by Lee et al. [13]. The open-to-air configuration enables rapid drying, evaporation, and solvent exchange; these are critical steps for no-carrier-added fluorination reactions, which are water-sensitive but begin with [^{18}F]fluoride ion obtained in [^{18}O]-enriched water from a cyclotron [4]. The low volumes (2-12 μL) used on the EWOD chip are conducive to simplifying the purification process and increasing specific activity (radioactivity per mass of tracer) due to the minute amount of reagents used in a single batch of synthesis [11, 22, 23].

Another potential advantage yet to be confirmed experimentally, is reduced radiolysis, which is damage to the reagents due to formation of radicals by energy that is mainly deposited from positron emission. Because the EWOD droplets are squeezed within a gap that is smaller than the positron range, it is expected that a significant portion of positrons will be absorbed in the chip substrate rather than solvent, which would significantly reduce the formation of radicals and radiolysis, in comparison with a macroscale geometry [24].

To avoid different chip designs for different tracers, in this report we explore and confirm a single EWOD chip design that could produce a variety of radiotracers, completing our preliminary efforts [22,25], along with significantly improved loading practices, shorter processing time, increased [^{18}F]fluoride concentration, and radiochemical yields. Four exemplary radiotracers currently used in

clinical and preclinical research are demonstrated: (1) [¹⁸F]FDG (a sugar analogue), (2) 3'-deoxy-3' [¹⁸F]fluorothymidine ([¹⁸F]FLT, a DNA nucleoside analogue), (3) N-succinimidyl 4- [¹⁸F]fluorobenzoate ([¹⁸F]SFB, a prosthetic group for protein labelling), and (4) [¹⁸F]fallypride (a neurotransmitter analogue). The EWOD platform, as an affordable and flexible synthesizer, has the potential to empower final users to produce tracers of their choice locally on demand and eliminate bottlenecks due to centralized production.

Experimental

Device description and fabrication

The EWOD chip has a configuration of two parallel plates with a gap space, in which droplets are sandwiched to a disk shape. The electrical ground plate is on top and uses a transparent conductive layer of indium tin oxide (ITO) to maintain a reference electrical connection for EWOD actuation. The actuation plate is on the bottom and has defined electrodes (also transparent ITO) for six droplet pathways that meet at a circular heating site (Fig. 1). The heating site consists of 4 concentric multifunctional electrodes [26], each a resistive element that can be used either for EWOD actuation of droplets (when voltage but no current is applied) or for feedback-controlled heating (when both voltage and current are applied). The multi-element heating site can center the droplet on the heater and maintain temperature more uniformly than a single-element heater [26,27] as the droplet shrinks during evaporations.

Both EWOD actuation plates and electrical ground plates were diced from 700 μm thick glass wafers coated with 140 nm ITO (Semiconductor Solutions). Chrome (20 nm) and gold (200 nm) were evaporated onto the wafers. The gold, chrome, and ITO layers were patterned to form EWOD electrodes, heaters, connection lines, and contact pads by photolithography and wet etching. The silicon nitride dielectric was deposited by plasma-enhanced chemical vapor deposition at a thickness of 2 μm on the actuation plate and a thinner 100 nm on the electrical ground plate. Teflon® (250 nm) was spin-coated and annealed at 340°C under vacuum to make the surfaces hydrophobic. A 140 μm gap between the assembled actuation plate and electrical ground plate was maintained by two layers of double-sided tape (3M Inc.).

The hydrophobic coating consisted of Cytop® (glass transition temperature $T_g = 108^\circ\text{C}$) in early devices [21,26], but was switched to Teflon® AF 2400 ($T_g = 240^\circ\text{C}$) in the current devices for its higher thermal stability. Teflon® AF 2400 was considered even more stable than Teflon® AF 1600 ($T_g = 160^\circ\text{C}$) used in the work preliminary to this report [22,25]. The highest temperature used in our radiolabelling is 120°C. After the hydrophobic topcoat was switched from Cytop® to Teflon® AF 2400, less residual radioactivity remained “stuck” to the chip surface after synthesis. Compared to the

initially loaded activity, the extracted product radioactivity has increased from 45% (in the preliminary work although not specifically reported in [22]) to 77% (decay-corrected) for [^{18}F]FLT synthesis.

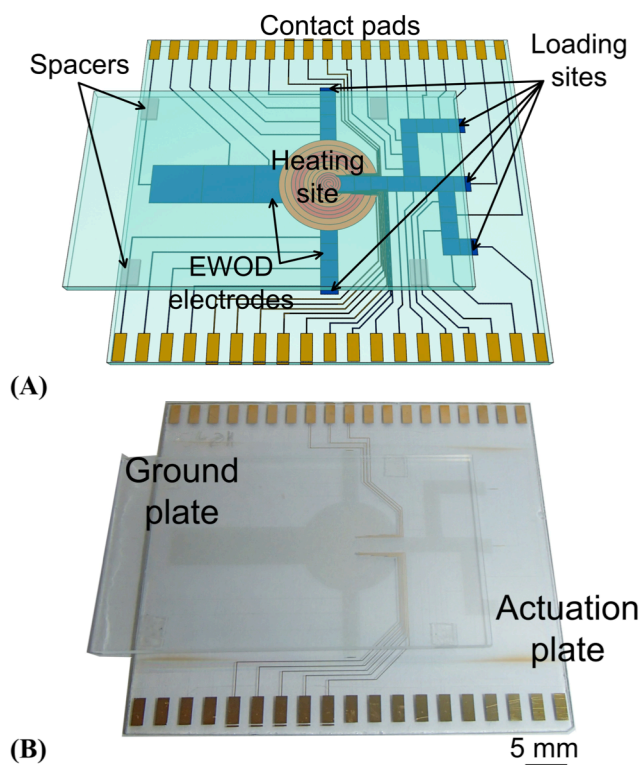


Fig. 1 EWOD chip designed and fabricated for tracer synthesis. (A) Schematic of the chip, showing the actuation glass plate patterned with regular EWOD electrodes (blue), multifunctional electrodes named heating site (orange and red), and electric contact pads along the two edges, as well as the electrical ground glass plate assembled on top, (B) A picture of the fabricated chip, showing the EWOD and multifunctional electrodes (slightly darker) and gold connection lines and contact pads (yellow).

One concern with Teflon® is that it can be a source for fluorine-19 contamination into the reagents and result in a lower specific activity of the final product [28]. However, because [^{18}F]fallypride synthesized by EWOD has some of the highest reported specific activity (19 Ci/ μmole), fluorine-19 contamination from Teflon® appears not likely to be a major issue [23].

Device operation

EWOD actuation voltage for droplet movement was generated from a 10 kHz signal (33220A waveform generator, Agilent Technologies) and amplified to 100 V_{rms} (Model 601C, Trek) (Fig. 2). The voltage was applied selectively to desired electrodes for droplet movement by solid-state relays (AQW610EH PhotoMOS relay, Panasonic) that were controlled by a LabVIEW program using a

digital I/O device (NI USB-6509, National Instruments).

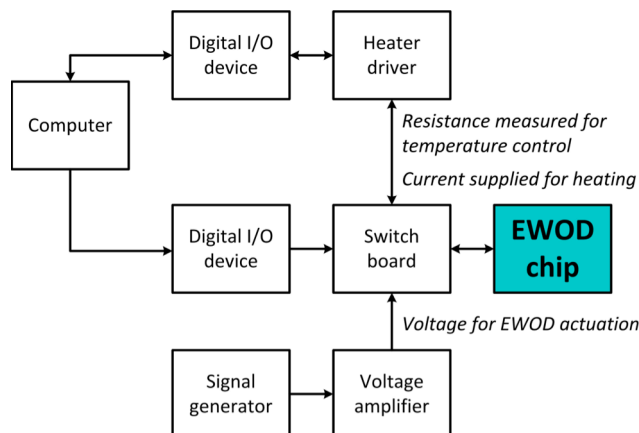


Fig. 2 Electronic control scheme to operate the EWOD chip for tracer synthesis. A computer controls a switchboard through a digital input/output device. The switches connect the electrodes on the EWOD chip to an amplified voltage for EWOD actuation. When necessary, some switches connect the multifunctional electrodes to a heater driver for temperature sensing and resistive heating via feedback control from the computer through a second digital input/output device.

A multichannel heater driver was designed and built in house and interfaced with a digital I/O device (NI USB-6343, National Instruments) to maintain feedback-controlled temperatures over the four individual resistive heaters on each actuation plate. The multifunctional electrodes were individually connected to a switch to alternate between EWOD actuation or temperature measurement and heating.

Reagents and materials

No-carrier-added [^{18}F]fluoride ion was obtained by irradiation of 97% [^{18}O]-enriched water with an 11 MeV proton beam using a cyclotron (RDS-112, Siemens, Knoxville, TN) at the UCLA Ahmanson Biomedical Cyclotron Facility.

Potassium carbonate (K_2CO_3 , 99%), 2,3-dimethyl-2-butanol (hexyl alcohol), anhydrous acetonitrile (MeCN, 99.8%), anhydrous dimethyl sulfoxide (DMSO, 99.9%), anhydrous methanol (MeOH, 99.8%), and *N,N,N',N'*-tetramethyl-*O*-(*N*-succinimidyl)uronium hexafluorophosphate (HSTU, 98%) were purchased from Sigma Aldrich. Hydrochloric acid (HCl, 1 N) and sodium hydroxide (NaOH, 1 N) were purchased from Fisher Scientific. Mannose triflate (FDG precursor), 4,7,13,16,21,24-hexaoxa-1,10-diazobicyclo (8.8.8)-hexacosane ($\text{K}_{2.2.2}$, 98%), tetrabutylammonium bicarbonate solution (75 mM) (TBAHCO_3), 3-*N*-Boc-5'-*O*-dimethoxytrityl-3'-*O*-nosyl-thymidine (FLT precursor), 4-(*tert*-butoxycarbonyl)-trimethylbenzeneammonium triflate (SFB precursor), and

tosyl-fallypride (fallypride precursor) were purchased from ABX Advanced Biochemical Compounds (Radeberg, Germany). All chemicals were used as received. A vortex mixer (Vortex Genie 2, Scientific Industries) was used for off-chip preparation of reagents.

Neutral alumina (50-300 μm particle size), C-18 resin (55-105 μm particle size), and hydrophilic-lipophilic-balanced resin were purchased from Waters (Milford, MA). Ion retardation resin (AG11 A8, 180-425 μm particle size) and cation exchange resin (AG-50W-X4, 63-150 μm particle size) were purchased from BioRad Laboratories (Hercules, CA).

Solvents and solutions commonly used for radiotracer synthesis were tested for EWOD compatibility. Repeatable movement, splitting, and merging of droplets was accomplished with MeCN, DMSO, MeOH, TBAHCO₃, TSTU, K₂CO₃ in water (1 M), HCl (1 N), and NaOH (1 N), with voltages below 80 V_{rms} and frequencies ranging 0-1 kHz.

Analytical methods

Radioactivity was measured from samples using a calibrated ion chamber (Capintec CRC-15R). Radio thin layer chromatography (radio-TLC) was analysed with a scanner equipped with scintillation probe for gamma rays (MiniGITA star, Raytest). High performance liquid chromatography (HPLC) was carried out on a reversed-phase C-18 column (250 x 4.6 mm, 5 μm , Phenomenex Luna) equipped with a variable wavelength UV detector and a radiation detector (Eckert&Ziegler).

Fluoride concentration

[¹⁸F]fluoride is delivered in [¹⁸O]-enriched water from the cyclotron and is mixed with base and phase transfer catalyst. In earlier work [21] including those preliminary to this report [25,26], the mixing was done off chip with a vortex mixer prior to loading onto the EWOD chip. For [¹⁸F]FDG and [¹⁸F]SFB radiolabeling in this work, mixing was instead performed on chip by EWOD actuation after loading solutions of base and phase transfer catalyst separate from [¹⁸F]fluoride onto the chip. After being loaded onto the electrical ground plate edge by using a micropipette, the 2-10 μL droplets were pulled in between the plates and moved to the circular multifunctional electrode site by EWOD actuation. The loading process was repeated until the desired volume was reached, upon which the mixed droplet was heated at 105°C to dry.

The amount of radioactivity loaded was initially restricted by the droplet volume that could be squeezed within the 140 μm gap over the 12 mm diameter heater site, limiting us to a maximum volume of 16 μL fluoride solution that could be reduced by evaporation [26]. More radioactivity can be used by repeated loading and heating steps, but this lengthens the synthesis time. Further development allowed us to concentrate larger volumes by not squeezing the initial droplet between the plates (i.e., into a disk shape) but instead loading and heating a much larger droplet on the open

surface of the bottom plate (i.e., in a spherical shape) near the edge of the top electrical ground plate, as shown in the top figure of Fig. 3a. Here, a 200 μL droplet of fluoride with base and phase transfer catalyst could be heated outside of the gap and then pulled between the gap by EWOD after its volume reduced to 5 μL (Fig. 3). Within the gap, the droplet could shrink more or be completely dried with further heating. The total heating time was 12 minutes, but the 10 minutes outside of cover plate could potentially be reduced with the addition of a heater outside of the cover plate, specifically for concentration. Calibrated ion chamber measurements before and after concentration showed that negligible radioactivity was lost during the whole process. This method of removing bulk water for radiotracer synthesis is different from the conventional method, in which [^{18}F]fluoride is typically trapped on a cartridge of anion exchange resin and then eluted off in a release solution. The concentration cartridge can both reduce evaporation time (if the release solution contains less water) and also remove impurities that are released by the cyclotron target. However, the ability to concentrate fluoride ion directly on the EWOD chip without using anion exchange resin provides an alternative means of preparing radiotracers with high specific activity. A recent report by Lu et al. [11] showed high fluorine-19 carrier contamination when the fluorine-18 solution was first concentrated with anion exchange resin.

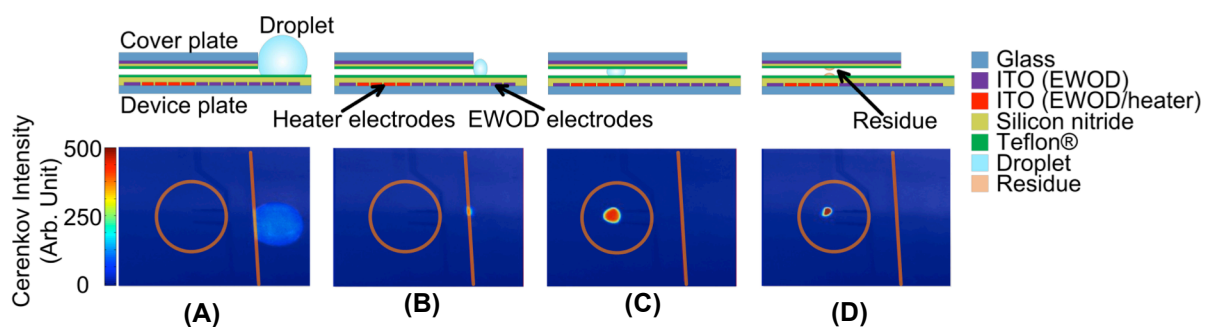


Fig. 3 Images of Cerenkov radiation emitted during fluorine-18 positron decay during fluoride concentration and cross-section schematics of the chip in corresponding stages. Cerenkov analysis of on-chip synthesis has been demonstrated by Dooraghi et al. [29]. In the Cerenkov images, red represents a higher concentration of radioactivity. Orange lines and circles were added to depict the cover plate edge and the heating site, respectively. (A) 200 μL droplet of [^{18}F]fluoride with base and phase transfer catalyst loaded to the cover plate edge (depicted with an orange line). (B) Droplet at cover plate edge after its volume was reduced by heating the nearby multifunctional electrodes to 150°C. (C) Droplet at center of heater after EWOD actuation. (D) Residue at the heater center after solvent evaporation.

Solvent exchange and azeotropic drying

Because of its open-to-air configuration, the EWOD chip facilitates evaporative removal of solvent, unlike many other types of microfluidic devices [30]. Solvent exchange is performed on the

EWOD chip by heating until the solvent has been evaporated and its vapours removed with a nitrogen stream, leaving behind a solute residue at the heater region. A droplet of the new solvent is loaded at the cover plate edge, and then EWOD actuation is used to pull the droplet in between the plates, move it to the residue site, and dissolve the residue.

For azeotropic drying, MeCN is added at the electrical ground plate edge, moved to the reactor site by electrowetting actuation, mixed, and heated at 105°C for 1 min. Due to the properties of the water-MeCN azeotrope, this is an effective method for removing residual water. Typically, fluorine-18 radiochemistry processes using the macroscale synthesizer include 2-3 successive cycles of azeotropic evaporation with MeCN to obtain the “naked” [¹⁸F]fluoride ion for the subsequent fluorination reaction [4]. Multiple azeotropic evaporations were also used in the preliminary devices [21,26] as well as our early work [22,25]. However, in the current microfluidic droplet synthesis, no significant improvements in reaction yields were found when increasing the number of azeotropic drying steps on the EWOD chip. Thus, only one azeotropic drying step was used, reducing the overall synthesis time and therefore radioactive decay.

Fluorination reaction

Fluorination was realized on the EWOD chip by first loading a precursor solution (Fig. 4). After electrowetting pulled the precursor droplet from the electrical ground plate edge and moved it to the dried fluoride, the heating site was heated to 105-120°C for 2-6 minutes depending on the type of radiotracer. For [¹⁸F]FDG, the 10 minute fluorination time used before [21] was reduced to 5 minutes in this report without a noticeable change in reaction yield.

Conventionally, nucleophilic radiofluorination reactions use MeCN as a solvent because its low boiling point (82°C) facilitates rapid removal by evaporation after the synthesis. Although many nucleophilic fluorination reactions have been reported to be more efficient in DMSO due to its high polarizability and ability to perform reactions at higher temperatures [31], DMSO is not typically used in macroscale synthesis because its low volatility (189°C boiling point) makes its evaporative removal difficult in a short time. However, microliter volumes of DMSO could be effectively evaporated at 120°C in the EWOD chip after fluorination. The remaining DMSO did not affect following reactions in the synthesis, and the residual amount after synthesis (870 ppm) was below the acceptable limits for human use (5,000 ppm) [21].

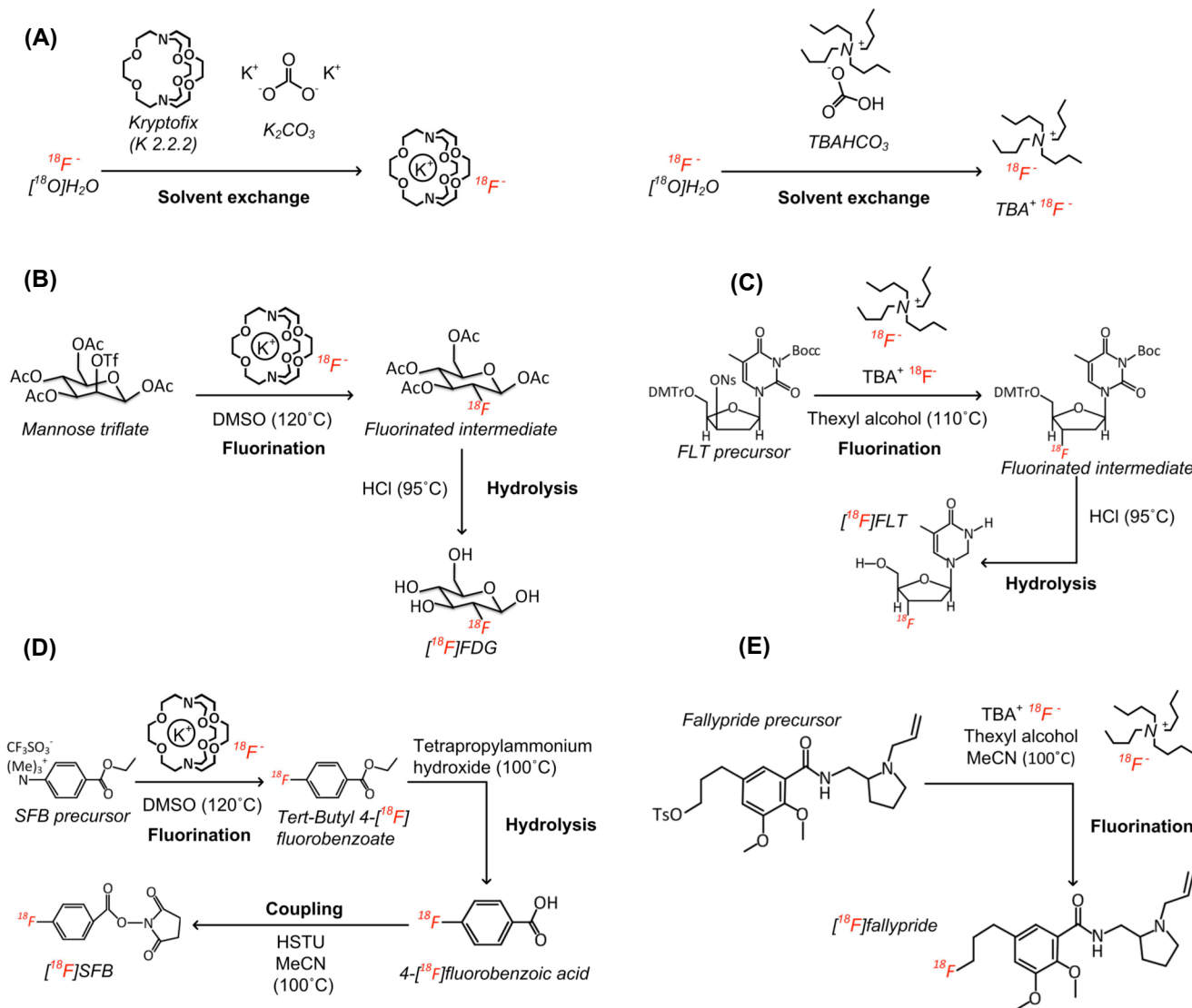


Fig. 4 Synthesis schemes for the four radiotracers produced on the EWOD chip. (A) Solvent exchange of fluoride with phase transfer catalyst. (B) Two-step synthesis of ^{18}F FDG. (C) Two-step synthesis of ^{18}F FLT. (D) Three-step synthesis of ^{18}F SFB. (E) One-step synthesis of ^{18}F fallypride.

Other reactions

Ideally, fluorine incorporation is the last synthesis step for radiotracer preparation in order to minimize the overall synthesis time and thus minimize the amount of radioactivity decay and reduce radiation exposure to the operator. A synthesis process with fewer steps is also inherently more reliable and simpler to automate. However, due to the high basicity of the “naked” fluoride ion, the majority of complex molecules require additional synthesis steps after fluorination, such as: removal of protecting groups (by acidic or alkaline hydrolysis), saponification, esterification, and coupling reactions.

To accomplish multistep reactions in the EWOD chip, the reagents were loaded from the

electrical ground plate edge and mixed with the previous reaction's products by electrowetting. The multifunctional electrodes were then heated to the set reaction temperature over a predetermined reaction time. All of the synthesis reactions were performed at the same heating site without any intermediate purification steps.

Although efforts were made to maximize individual isolated pathways for loading reagents, the synthesis results were not affected in tests where the same route was used for all reagents. This was the case, even if a reagent was water sensitive and followed the same path as an aqueous reagent. Contamination from adsorption was not an issue, because all of the radiotracer processes demonstrated involved a one-pot synthesis and only one reactor site was used on chip. Also, there was very limited radioactive residue on the chip during droplet routing based on previous work using Cerenkov imaging for analysis [29]. However, residue became significant on the reactor site after heating.

Radio-TLC was used to analyse the reaction efficiencies after crude reaction mixtures were spotted onto silica gel plates and developed in appropriate mobile phases. Multiple peaks were visible in each TLC chromatogram, one corresponding to the desired reaction product and the other(s) to unreacted starting material and/or byproducts. The reaction efficiency was determined from the area under the product peak divided by the total area under all peaks. For radiotracer synthesis processes requiring multiple reactions, the combined reaction efficiency was the multiplied product of all the individual reaction efficiencies. Radio-TLC was also used to measure radiochemical purity of the purified product.

Extraction

The final reaction mixture from the EWOD chip was manually extracted by pipette after removing the electrical ground plate and washing both plates with solvent (i.e., MeCN, DMSO, MeOH, H₂O). An automated approach was also tested, in which the crude product droplet were moved away from the reactor after synthesis reactions to an outlet droplet pathway by EWOD actuation, and then pulled off chip into a vial by vacuum. An additional 3-6 μ L solvent was required to move the product droplets away from the heating site for [¹⁸F]FDG, [¹⁸F]FLT, and [¹⁸F]fallypride, but no additional solvent was required for [¹⁸F]SFB.

Radioactivities of the [¹⁸F]fluoride complex solution before and after loading, the total EWOD chip after the synthesis, the extracted product, actuation plate, electrical ground plate, and pipette tips were measured with a calibrated ion chamber. The extraction efficiency was determined by dividing the radioactivity of the crude product droplet after extraction by the post-synthesis radioactivity of the total EWOD chip before extraction.

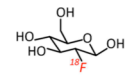
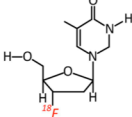
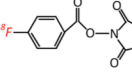
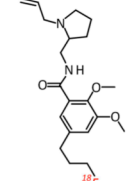
Purification and analysis

The crude reaction mixtures were purified off chip to isolate the desired radiotracer from unreacted reagents, intermediates, and by-products, which are not safe to be administered into animals and patients, and can complicate interpretation of images if the by-products are radioactive. Two different purification methods were used depending on the type of radiotracer.

[¹⁸F]FDG and [¹⁸F]FLT were purified via a solid phase extraction (SPE) method using miniaturized cartridges prepared in-house. Each cartridge contained 4 types of SPE sorbents. For [¹⁸F]FDG purification, neutral alumina, ion retardation, cation exchange, and C-18 sorbents removed impurities as the crude radiotracer mixture was pushed into the cartridge and the purified radiotracer was outputted. For [¹⁸F]FLT purification, neutral alumina, ion retardation, and cation exchange sorbents were also used, but C-18 was replaced with hydrophilic-lipophilic-balanced resins to retain [¹⁸F]FLT as impurities from the crude radiotracer were outputted from the cartridge into waste. The desired [¹⁸F]FLT radiotracer was then eluted as a purified product in ethanol.

HPLC was used to purify [¹⁸F]SFB and [¹⁸F]fallypride, as the final radiotracer and other impurities were difficult to be purified via solid phase extraction. Due to the small quantities of reagents used, the mass of impurities is much lower from the EWOD chip than conventional systems, and thus an analytical-scale HPLC column was sufficient for preparative use. A separate analytical

Table 1 Four diverse radiotracers synthesized using the same EWOD chip design.

| Tracer | Molecule | Application | Radiopharmacy availability | Fluorination efficiency ¹ | Combined reaction efficiency ¹ | Extraction efficiency ¹ | Before-purification yield ^{1,2} | Synthesis Time ³ | Radiochemical Yield ¹ |
|---|---|---------------------------|----------------------------|--------------------------------------|---|------------------------------------|--|-----------------------------|----------------------------------|
| [¹⁸ F]fluoro-2-deoxy-D-glucose ([¹⁸ F]FDG) |  | Sugar metabolism | Yes | 93% ± 3% (n=2) | 93% ± 3% (n=2) | 63% ± 8% (n=2) | 45% ± 10% (n=2) | 50 ± 3 min (n=2) | 37 ± 13% (n=2) |
| 3'-deoxy-3'-[¹⁸ F]fluorothymidine ([¹⁸ F]FLT) |  | DNA proliferation | Limited | 95% ± 3% (n=6) | 95% ± 3% (n=6) | 81% ± 5% (n=6) | 74% ± 7% (n=6) | 40 ± 4 min (n=6) | 56% ± 8% (n=6) |
| 4-[¹⁸ F]fluorobenzoate ([¹⁸ F]SFB) |  | Protein labeling | No | 90% ± 6% (n=5) | 85% ± 5% (n=3) | 80% ± 17% (n=3) | 34% ± 10% (n=3) | 58 ± 8 min (n=3) | 19% ± 8% (n=5) |
| [¹⁸ F]fallypride |  | Neuro-transmitter binding | No | 90% ± 9% (n=6) | 90% ± 9% (n=6) | 94% ± 3% (n=6) | 84% ± 7% (n=6) | 31 ± 1 min (n=6) | 65% ± 11% (n=6) |

¹All reported efficiencies and yields have been corrected for radioactive decay.

²Before-purification yield was the extracted radioactivity multiplied by the combined reaction efficiency and divided by the loaded radioactivity.

³Synthesis time was from start of loading to end of extraction.

HPLC system was used to test the chemical and radiochemical purity for all of the synthesized radiotracers after purification.

While we used fluorination efficiency and hydrolysis efficiency to characterize radiotracer synthesis for the preliminary results [22,25], in this report we demonstrated the entire PET probe production process starting from synthesis, and including purification and reformulation. Here we report the final decay corrected radiochemical yield obtained after the purification and reformulation in saline. The final radiochemical yield was determined by comparing the decay-corrected radioactivity of the purified product with the initial fluoride radioactivity loaded onto the chip for synthesis.

Results and discussion

Radiotracer synthesis yield

Upon setting the main reaction parameters of reagent, concentration, temperature, and time, the reaction efficiencies for each radiotracer synthesis process were reliable and generally high (Table 1). The four example tracers demonstrated here include both aliphatic nucleophilic fluorination reactions as well as aromatic nucleophilic fluorination, which generally require harsher reaction conditions. Compared with preliminary results [22,25], the fluorination efficiency has improved from 80% to 90% or greater for all four tracers. Purified radiochemical yield for all four tracers is presented for the first time on the right-most column of Table 1.

As summarized in the 6th column of Table 1, the combined reaction efficiency (decay corrected) was $93\% \pm 3\%$ (n=2) for [^{18}F]FDG, $95\% \pm 3\%$ (n=6) for FLT, $85\% \pm 5\%$ (n=3) for [^{18}F]SFB, and $90\% \pm 9\%$ (n=6) for [^{18}F]fallypride. These reaction efficiencies were comparable to or exceeded macroscale methods.

Extraction efficiency varied with each radiotracer's synthesis: $63\% \pm 8\%$ (n=2) for [^{18}F]FDG, $81\% \pm 5\%$ (n=6) for [^{18}F]FLT, $80\% \pm 17\%$ (n=3) for [^{18}F]SFB, and $94\% \pm 3\%$ (n=6) for [^{18}F]fallypride. Although the extraction efficiency was comparable with other microfluidic synthesizers, it was poor compared to macroscale synthesizers where extraction efficiency is typically greater than 95%. During the extraction step, 0-3% of the radioactivity was lost to the pipette tip and the remaining radioactivity was left on the actuation and cover plates.

Before-purification yields were determined by multiplying combined reaction efficiency by measured extraction radioactivity and dividing it by the initially loaded radioactivity. Compared with the before-purification yields presented in [25] (50% for [^{18}F]FLT and 72% for [^{18}F]fallypride), the current before-purification yields (73% for [^{18}F]FLT and 84% for [^{18}F]fallypride) have improved by 45% for [^{18}F]FLT and 16% for [^{18}F]fallypride.

The EWOD chip can use different solvents and shorter reaction times than conventional synthesizers, but because it is open to air, care must be taken to not lose radioactivity as volatile side products and intermediates. Also because the reactor was not sealed, the droplet size reduced during heating, even if the temperature was below the boiling point. Attempts were made to keep a stable concentration by replenishing the volume with smaller solvent droplets, but we found that the reaction yields were higher with shorter heating times when the droplet size was reduced, which resulted in an overall increase in the concentration of the reagents [21].

Although reaction times are typically shorter when performed with microfluidic volumes [4], the overall radiotracer synthesis time (from initial loading to extraction) on the EWOD device was longer than desired and ranged from 31 ± 1 min for [^{18}F]fallypride (n=6) to 58 ± 8 min for [^{18}F]SFB (n=3). During the developmental period, the synthesis times were longer due to tedious process of manual reagent loading and manual activation of electrodes. The overall synthesis time is anticipated to be reduced with integrated reagent delivery and further automation in the electrowetting and heating control [32].

Conclusions

We have developed an EWOD radiosynthesizer in an effort to create an affordable and flexible platform to enable researchers and clinicians to produce their own tracer of interest on demand. To demonstrate the success of the effort, we have successfully performed several classes of radiochemical reactions (including aliphatic nucleophilic substitution, aromatic nucleophilic substitution, hydrolytic deprotection, saponification, and esterification) using one EWOD chip design. Our goal is a universal chip that can produce the radiotracer of choice as long as reagents are provided. A mass-produced universal chip may be disposable and fresh for each radiosynthesis, allowing imaging centers to produce multiple, different radiotracers back-to-back by simply swapping the chips and reagents.

To date, [^{18}F]FDG and [^{18}F]NaF are the only two radiotracers that are routinely available from commercial radiopharmacies. Other PET tracers are highly expensive or only available from specialized radiochemistry facilities. Several research groups have advanced microfluidic radiosynthesizer technology in recent years, and the first microfluidic device for clinical production of human doses of ^{18}F -labeled PET tracers was presented in early 2013 [30].

The EWOD radiosynthesizer is distinctive as the only batch reactor using droplets in air or an inert gas, which provides unique advantages in its flexibility for radiosynthesis (because fluid paths are software-programmable) and greatly facilitates evaporation steps. The EWOD radiosynthesizer

also has the potential to produce radiotracers with unprecedented high specific radioactivity. We will investigate various parameters in the microdroplet radiochemistry on EWOD chip to further understand the factors that influence specific activity and develop a generic EWOD radiosynthesizer to synthesize radiotracers with ultrahigh specific activity.

Acknowledgements

This work was supported in part by the UCLA Foundation from a donation made by Ralph & Marjorie Crump for the UCLA Crump Institute for Molecular Imaging and the Department of Energy [DE-SC0005056]. We thank Prof. David Stout for use of radiolabeling facilities, Dr. Wyatt Nelson for developing the multi-functional EWOD electrodes, Alex Dooraghi and Prof. Arion Chatziioannou for developing the Cerenkov setup, and Prof. Saman Sadeghi and Bob Silverman for developing the multi-channel temperature controller and software.

References

- [1] M.E. Phelps, *Proc. National Academy of Sciences*, 2000, 97, 9226-9233.
- [2] K. Serdons, A. Verbruggen, and G.M. Bormans, *Methods*, 2009, 48, 104-11.
- [3] A.M Elizarov, *Lab on a Chip*, 2009, 9, 1326-1333.
- [4] L.S. Cai, S.Y. Lu, and V.W. Pike, *Eur J Org Chem*, 2008, 17, 2853-2873.
- [5] R. Iwata, *Radiosynthesis database of PET probes*, National Institute of Radiological Sciences, Japan, 2013. Retrieved from <http://www.nirs.go.jp/research/division/mic/db2/>
- [6] C.H. Hsieh, *Positron Emission Tomography – Current Clinical and Research Aspects*, InTech, New York, United States, 2012, pp. 153-182.
- [7] E. Webster, M.S. Haka, and P. Gutierrez, et al., *J of Labelled Compounds & Radiopharmaceuticals*, 2011, 54, S438.
- [8] R. Krasikova, in *PET Chemistry – The Driving Force in Molecular Imaging*, Springer, Berlin, 2007, chapter 11, pp. 289-316.
- [9] G. Pascali, P. Watts, and P.A. Salvadori, *Nuclear Medicine and Biology*, 2013, 40, 776-787.
- [10] C. Rensch, A. Jackson, S. Lindner, R. Salvamoser, V. Samper, S. Riese, P. Bartenstein, C. Wangler, and B. Wangler, *Molecules*, 2013, 18, 7930-7956.
- [11] S.Y. Lu, A.M. Giamis, and V.W. Pike, *Curr Radiopharm*, 2009, 2, 49-55.
- [12] M. Yu, J. Matteo, D. Townsend, and R. Nutt, *J. Nuclear Medicine*, 2006, 47, 159P.
- [13] J. Lee, H. Moon, J. Fowler, T. Schoelhammer, and C.-J. Kim, *Sensors and Actuators*, Vol A95, 2002, 259-268.
- [14] K. Choi, A.H.C. Ng, R. Fobel, and A.R. Wheeler, *Annu Rev Anal Chem*, 2012, 5, 413-440.
- [15] M.J. Jebrail, M.S. Bartsch, and K.D. Patel, *Lab on a Chip*, 2012, 12, 2452-2463.
- [16] W. Nelson and C.-J. Kim, *J Adhesion Sci Tech*, 2012, 26, 1747-1771.
- [17] S.K. Cho, H.J. Moon, and C.-J. Kim, *J. Microelectromechanical Sys*, 2003, 12, 70-80.
- [18] J. Gong and C.-J. Kim, *Lab on a Chip*, 2008, 8, 898-906.
- [19] S. Sadeghi, H.J. Ding, G.J. Shah, S. Chen, P.Y. Keng, and C.-J. Kim, and, R.M. van Dam, *Analytical Chemistry*, 2012, 84, 1915-1923.
- [20] D. Witters, N. Vergauwe, R. Ameloot, S. Vermeir, D. De Vos, R. Puers, B. Sels, and J. Lammertyn, *Advanced Materials*, 2012, 24, 1316-1320.

- [21] P.Y. Keng, S. Chen, H.J. Ding, S. Sadeghi, G.J. Shah, A. Dooraghi, M.E. Phelps, N. Satyamurthy, A.F. Chatziioannou, C.-J. Kim, and R.M. van Dam, *Proc. National Academy of Sciences*, 2012, 109, 690-695.
- [22] S. Chen, R. Javed, J. Lei, H.-K. Kim, G. Flores, R.M. van Dam, P.Y. Keng, and C.-J. Kim, *Tech. Dig. Solid-State Sensor and Actuator Workshop*, Hilton Head Island, SC, United States, 189-192, (2012).
- [23] M.R. Javed, S. Chen, J. Lei, J. Collins, M. Sergeev, H.-K. Kim, C.-J. Kim, R.M. van Dam, and P.Y. Keng, *Chemical Communications*, 2014, 50, 1192-1194.
- [24] C. Rensch, B. Waengler, A. Yaroshenko, V. Samper, M. Baller, N. Heumesser, J. Ulin, S. Riese, and G. Resichl, *Applied Radiation and Isotopes*, 2012, 70, 1691-1697.
- [25] H.K. Kim, S. Chen, R. Javed, J. Lei, C.-J. Kim, P.Y. Keng, and R.M. van Dam, *Proc. Int. Conf. Miniaturized Systems for Chemistry and Life Sciences*, Okinawa, Japan, 617-619, (2012).
- [26] S. Chen, P.Y. Keng, G.J. Shah, R.M. van Dam, and C.-J. Kim, *Proc. Int. Conf. MEMS*, Cancun, Mexico, 980-983, (2011).
- [27] W.C. Nelson, I. Peng, G.-A. Lee, J.A. Loo, R.L. Garrell, C.-J. Kim, *Anal. Chem.*, 2010, 82, 9932-9937.
- [28] M.S. Berridge, S.M. Apana, and J.M. Hersh, *J of Labelled Compounds & Radiopharmaceuticals*, 2009, 52, 543-548.
- [29] A.A. Dooraghi, P.Y. Keng, S. Chen, M.R. Javed, C.-J. Kim, A.F. Chatziioannou, R.M. van Dam, *Analyst*, 2013, 138, 5654-5664.
- [30] A. Lebedev, R. Miraghai, K. Kotta, C.E. Ball, J. Zhang, M.S. Buchsbaum, H.C. Kolb, and A. Elizarov, *Lab on a Chip*, 2013, 13, 136-145.
- [31] A.J. Parker, *Chemical Review*, 1969, 69, 1-32.
- [32] G.J. Shah, H.J. Ding, S. Sadeghi, S. Chen, C.-J. Kim, and R.M. van Dam, *Lab on a Chip*, 2013, 13, 2785-2795.

Radiolabelling diverse positron emission tomography (PET) tracers using a single digital microfluidic reactor chip

Supin Chen,^a Rashed Javed,^{bc} Hee-Kwon Kim,^{‡bc} Jack Lei,^{bc} Mark Lazari,^{abc} Gaurav J. Shah,^{bcd} R. Michael van Dam,^{abc} Pei-Yuin Keng,^{bc} and Chang-Jin “CJ” Kim^{ae}

^a Bioengineering Department, University of California, Los Angeles, CA 90095, USA.

^b Molecular and Medical Pharmacology, University of California, Los Angeles, CA 90095, USA

^c Crump Institute for Molecular Imaging, University of California, Los Angeles, CA 90095, USA

^d Sofie Biosciences, Culver City, CA 90230, USA

^e Mechanical and Aerospace Engineering, University of California, Los Angeles, CA 90095, USA

[‡]Current affiliation: Department of Nuclear Medicine, Molecular Imaging & Therapeutic Medicine Research Center, Biomedical Research Institute, Chonbuk National University Medical School and Hospital, Jeonju, Jeonbuk 561-712, South Korea.

Radiochemistry requires lead shielding to protect users from harmful radiation. For convenience, a standard radiochemistry “L-block” table shield was used as the main shielding. Further development can reduce the shielding size as it should only be necessary to house the chip and reagents.

It is possible to monitor the on chip radioactivity distribution by imaging Cerenkov radiation [1]. Cerenkov radiation is light that is produced when a beta particle travels faster than the speed that light travels in the surrounding medium. Because the EWOD chip gap (140 μm) is less than the average positron range (1.0 mm in water) most of the beta particles emitted by fluorine-18 are expected to travel through the transparent glass substrate (each plate is 0.7 mm thick), through which they can travel at a faster speed than light would travel in the glass. The emitted Cerenkov radiation is in the UV and visual spectrum and can be detected by a sensitive camera.

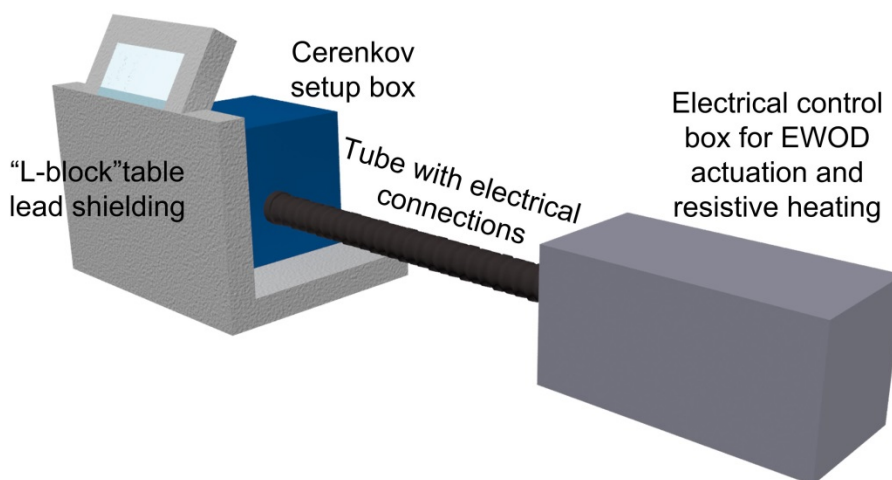


Fig. S11 Shielding and System-Setup. The “L-block” table shields the Cerenkov setup which is contained in a light-tight box and holds the EWOD chip. Electrical connections to the chip, mirror control, and cameras are passed along ribbon cables in a tube to reduce light exposure into the Cerenkov setup. The electrical control box contains a waveform generator, voltage amplifier, solid-state relays, a multichannel heater driver, and two digital I/O devices. The waveform generator creates a voltage signal that is amplified for EWOD actuation. Solid-state relays controlled

Supplementary Information

by a digital I/O device selectively connect the EWOD actuation voltage to the desired EWOD electrodes. The second digital I/O device controls the multichannel heater driver.

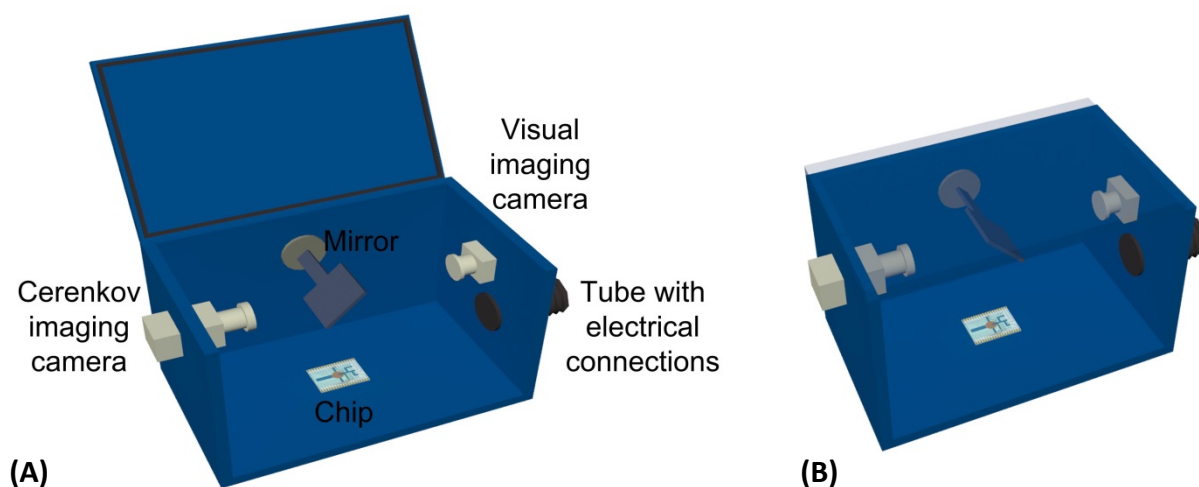


Fig. SI2 Cerenkov imaging setup. The Cerenkov imaging setup presented here is the same used by Dooraghi et al. [1]. It is housed in a light-tight box with a hinged lid that can close over a gasket. The chip was connected to electrical connections placed in the bottom of the box. A mirror was held on a motorized rotation stage above the chip to direct light into one of two cameras. One camera (DFK 21AU04, Imaging Source, Charlotte, NC) was used for standard visible imaging to remotely monitor the on chip processes. The second camera (QSI 540, Quantum Scientific Imaging, Poplarville, MS) was more sensitive and used for imaging Cerenkov radiation. Electrical connections were fed into the box through a tube to minimize interference from exterior light. (A) During regular EWOD operation, the lid was open and the mirror reflected the chip towards the visual imaging camera. (B) To image the on chip radioactivity, the lid was manually closed and the motorized stage directed the mirror towards the Cerenkov imaging camera.

[1] A.A. Dooraghi, P.Y. Keng, S. Chen, M.R. Javed, C.-J. Kim, A.F. Chatziioannou, R.M. van Dam, *Analyst*, 2013, 138, 5654-5664.